SCIENTIFIC REPORTS

OPEN

SUBJECT AREAS:
MYELODYSPLASTIC SYNDROME
TARGETED THERAPIES

Received
17 September 2014

Accepted
12 November 2014

Published
4 December 2014

Correspondence and requests for materials should be addressed to X.L. (lixiao3326@163.com)

Rigosertib as a selective anti-tumor agent can ameliorate multiple dysregulated signaling transduction pathways in high-grade myelodysplastic syndrome

Feng Xu, Qi He, Xiao Li, Chun-Kang Chang, Ling-Yun Wu, Zheng Zhang, Li Liu, Wen-Hui Shi, Yang Zhu, You-Shan Zhao, Shu-Cheng Gu, Cheng-Ming Fei, Juan Guo, Dong Wu & Liyu Zhou

Department of Hematology, Shanghai Jiao Tong University Affiliated Sixth People's Hospital.

Rigosertib has demonstrated therapeutic activity for patients with high-risk myelodysplastic syndrome (MDS) in clinical trials. However, the role of rigosertib in MDS has not been thoroughly characterized. In this study, we found out that rigosertib induced apoptosis, blocked the cell cycle at the G2/M phase and subsequently inhibited the proliferation of CD34+ cells from MDS, while it minimally affected the normal CD34+ cells. Further studies showed that rigosertib acted via the activation of the P53 signaling pathway. Bioinformatics analysis based on gene expression profile and flow cytometry analysis revealed the abnormal activation of the Akt-PI3K, Jak-STAT and Wnt pathways in high-grade MDS, while the p38 MAPK, SAPK/JNK and P53 pathways were abnormally activated in low-grade MDS. Rigosertib could markedly inhibit the activation of the Akt-PI3K and Wnt pathways, whereas it activated the SAPK/JNK and P53 pathways in high-grade MDS. A receptor tyrosine kinase phosphorylation array demonstrated that rigosertib could increase the activation of RET and PDGFR-β while reducing the activation of Tie2 and VEGFR2 in MDS cells. Taken together, these data indicate that rigosertib is a selective and promising anti-tumor agent that could ameliorate multiple dysregulated signaling transduction pathways in high-grade MDS.

Myelodysplastic syndromes (MDS) encompass a class of clonal diseases characterized by the abnormal maturation and differentiation of hematopoietic cells and a high risk of progression to leukemia[1]. Due to the complexity and heterogeneity of the pathogenesis of MDS, therapeutic agents approved for MDS remain scarce. Decitabine and 5-azacitidine have shown therapeutic activity, although response rates are relatively low, and the resultant prolongation in survival was limited and unsatisfactory[2,3]. Almost all patients who initially respond to hypomethylating agents become unresponsive in a short period or eventually progress into AML[4]. Thus, new agents should be developed to treat MDS.

Rigosertib is a novel non-ATP competitive anticancer agent that inhibits mitotic progression and induces apoptosis in solid cancer cells and lymphoma cells, while it rarely affects normal cells[5–8]. Several studies have revealed that rigosertib exerts anti-tumor activity by inhibiting the PLK1 and Akt-PI3K pathway[5,6,9]. In various tumor xenograft mouse models, including human liver, breast, and pancreatic cancer models, rigosertib did not only show promising anti-tumor activity but also showed a low toxicity profile with rare hematotoxicity[5]. Rigosertib has also shown therapeutic activity and drug tolerance in patients with solid tumors in a phase I oral study[9,10]. In hematopoietic malignancies, rigosertib was first applied to treat MDS[11–13]. In a recent phase I/II clinical trial with oral rigosertib treatment, 4 of 13 higher risk MDS patients unresponsive to hypomethylating therapy achieved a marrow complete response, and 8 of the remaining 9 patients had stable disease, which is associated with good drug tolerance[11]. In another phase II clinical trial, intravenous rigosertib was well tolerated and showed favorable clinical activity in patients with higher risk MDS[13]. However, the mechanism of action of rigosertib in MDS is not well described. Because rigosertib is a kinase inhibitor, the relationship between rigosertib and signaling transduction pathways in MDS merits further investigation. In this study, we analyzed the effect of rigosertib on the tumor biology and signaling transduction pathways of MDS cells. This study aimed to elucidate the mechanism of action of rigosertib and to determine a kinase biomarker for rigosertib treatment.

Methods

Antibodies and reagents. The following antibodies were used for flow cytometry analysis: Anti-Akt1-PE, anti-ERK1/2 (pT202/pY204)-PE, anti-STAT1 (pY701)-VioBlue and anti-CD34- APC were purchased from Miltenyi Biotec (Shanghai, China). Anti-Akt (pS473)-PE, anti-STAT3 (pY705)-Alexa fluor 488, anti-p38 MAPK (pT180/pY182)-Alexa fluor 488, anti-SAPK/JNK (pT183/pY185)-PE, anti-β-Catenin (pS45)-PE, anti-p53 (pS37)-Alexa fluor 488, anti-PLK (pT210)-PE, anti-p53-PE, anti-bcl-2-PE, anti- cleaved Caspase-3-FITC and anti- Cyclin D1-FITC were purchased from BD Pharmingen (Shanghai, China). Anti-$P21^{Waf1/Cip1}$-PE, anti-cleaved PARP- Alexa fluor 488 and anti-Cyclin B1-Alexa Fluor 488 were purchased from Cell Signaling Technology (Shanghai, China). Rigosertib and decitabine were purchased from Selleck Inc. (Shanghai, China). Both reagents were dissolved in DMSO with a concentration of 10 mM. In a series of experiments, CD34+ cells and cell lines were incubated with 0.5–20 μM rigosertib or 5 μM decitabine in the maintenance medium.

Patients and isolation of CD34+ cells. MDS was diagnosed in accordance with the minimum diagnostic criteria (Vienna, 2006)[14]. The classification and prognostic risk scoring of MDS were performed according to the WHO criteria and the revised International Prognostic Scoring System (IPSS)[15,16]. Detailed information about MDS patients is shown in Table 1. In addition, 13 healthy volunteers were defined as a normal control group. All subjects provided informed consent in accordance with the Declaration of Helsinki. The research was approved by the ethics committee of the Sixth Hospital affiliated with Shanghai Jiao Tong University. CD34+ cells were isolated by magnetic-activated cell sorting (MACS) from Bone marrow mononuclear cells according to the manufacturer's protocol. The yield and purity of the positively selected CD34 cells were evaluated by flow cytometry (FACS Calibur, Becton Dickinson). Usually, approximately $1–5 \times 10^6$ CD34+ cells from MDS patients were acquired and perform a series of biological experiments except for western blot analyses. Sometimes, $1–5 \times 10^6$ CD34+ cells from 2–3 MDS or normal samples were pooled because of insufficiency of CD34+ cells in single case.

Cell lines and culture. MDS-L cells were gifted from Prof. Tohyama[17]. SKM-1 cells were gifted from Prof. Nakagawa[18]. The leukemia cell lines, including K562, KG1a, Kasumi-1 and U937 cells, were obtained from ATCC. Cell lines were maintained in complete medium (RPMI 1640 supplemented with 10% heat-inactivated fetal bovine serum, 1% glutamine, and 1% sodium pyruvate). In addition, IL-3 (100 U/ml) is essential for MDS-L cells. However, MDS-L cells were maintained in complete medium without IL3 when treated with rigosertib in order to avoid the interference of IL-3 on cell signaling pathways. When treatment with rigosertib, CD34+ cells were cultured in serum-free SFEM medium (StemSpan, StemCell Technologies) without hematopoietic support factors except in proliferation assay.

Apoptosis detection. 5×10^4 cells with CD34+ and cell lines were exposed to increasing concentrations of rigosertib ranging from 0.5 μmol/L to 20 μmol/L for 24 hours. Apoptosis was evaluated by flow cytometry after staining with anti-Annexin V–FITC and PI (BD Pharmingen). The half lethal dose (LD50) was calculated using the SPSS software according to the percentage of apoptotic cells stained with Annexin V. To detect intracellular proteins, 10^5 cells were fixed with 4% paraformaldehyde, permeabilized with saponin 0.1%, stained for 45 minutes with 10 μL of fluorescence antibodies at room temperature, and then analyzed in FACS Calibur.

WST-1 proliferation assay. The cells were plated in 96-well plates at a density of 5×10^3 cells/well in triplicate and treated with rigosertib for 12–60 hours. For primary CD34+ cells from MDS patients and normal controls, pre-mixed cocktail of recombinant human cytokines (FLT3-Ligand, SCF, IL-3 and IL-6) (StemCell Technologies) were added into culture medium. After culture, ten microliters of WST-1 working solution (Keygen, Nanjing, China) was added to each well, and the cells were incubated for 2 hours. The absorbance at 450 nm was measured using a microplate reader. The inhibition rate of cell proliferation was calculated as follows: % of inhibition rate= each time point ($OD^{treated\ well}$- $OD^{blank\ well}$)/original point ($OD^{unreated\ well}$- $OD^{blank\ well}$).

Cell cycle analysis. 5×10^4 cells were washed with cold PBS, fixed in 70% ethanol, washed with PBS once more, and then re-suspended in 1 mL of PI staining reagent (50 mg/ml propidium iodide and 1 mg/ml RNAse). Samples were incubated in the dark for 30 min before cell cycle analysis. The cell cycle was measured with FACS Calibur. The percentages of cells in the G1, S and G2 phases were calculated with the Cellquest software.

Mitochondrial membrane potential detection. 10^5 cells were collected and suspended in fresh medium. After the addition of 0.5 mL of JC-1 working solution, the cells were incubated in a CO_2 incubator for 20 minutes. The staining solution was removed by centrifugation, and the cells were washed twice with JC-1 staining buffer. The change in the mitochondrial membrane potential was analyzed using FACS Calibur.

Western Blotting. MDS-L and SKM1 cells (10^7) were lysed with cell lysis buffer. Total cell extracts were fractionated on 10% sodium dodecyl sulfate polyacrylamide gels, electroblotted to polyvinylidene difluoride membranes (Millipore, Billerica, MA), and reacted with primary antibodies including Bax, Bcl-2, cleaved caspase-9, p-p53, CDK1, p-CDC25C, Cyclin B1, Cylin D1, p38 MAPK, p-p38 MAPK, p44/42, p-p44/42, SAPK/JNK, p-SAPK/JNK, Akt, p-Akt, GSK-3α/β, p-GSK- 3α/β and GAPDH (purchased from Cell Signaling Technology). Immunoreactivity was determined using the enhanced chemiluminescence method (Pierce Chemical, Rockford, IL).

RNA preparation and gene expression microarray (GEM). The total RNA was extracted from 10^5 CD34+ cells using the RNeasy system (Qiagen, Valencia, CA) following the manufacturer's instructions. A Genechip Primeview Human Gene Expression Array (Affymetrix, US) was used for the GEM study. The signal intensities were acquired with a Genechip Scanner 3000 7G (Affymetrix) to generate cell intensity files (CEL). The statistical analysis was performed using the Partek Genomics Suite software (Partek Inc., St. Louis, MO, USA). A robust multi-array average (RMA) algorithm was used to normalize the data. The false discovery rate (FDR) was less than 0.15 to minimize the false identification of genes. Changes greater than 2-fold were analyzed for up- or down-regulated genes. Hierarchical clustering based on genes and samples was performed with the Cluster 3.0 software.

Pathway and Pathway-net analysis of differentially expressed genes. Pathway analysis was utilized to determine the significant pathway based on the differential genes according to KEGG. Fisher's exact test was used to select the significant pathway, and the threshold of significance was defined by the P-value and FDR. The Path-Net was the net interaction of the significant pathways of the differential expression genes and was built according to the interaction among the pathways of the KEGG database to directly and systemically determine the interaction among the significant pathways. This approach could summarize the pathway interaction of genes differentially expressed in diseases and identified why a certain pathway was activated.

Flow cytometry analysis of signal pathway protein. Heparin anticoagulant marrow solutions were labeled with anti-CD34-APC at room temperature for 15 minutes and then treated with a lysing solution and a permeabilizing solution. Next, the cells were stained with a series of intracellular fluorescence antibodies at room temperature for 45 minutes. The expression or phosphorylation of signal pathway proteins in CD34+ cells was quantified based on the mean fluorescence intensity (MFI). All clinical samples underwent FCM analysis within 6 hours. A FACS Calibur equipped with the CellQuest software was used for logarithmic (Log) sampling, in which at least 10^5 total cells and 1000 CD34+ cells were acquired and analyzed for most samples.

RTK phosphorylation array. MDS-L and SKM1 cells were treated with 5 μM of rigosertib or DMSO for 12 hours and then harvested in protein lysis buffer. The Human RTK phosphorylation Antibody Array assay (RayBiotech, Inc) was carried out according to the manufacturer's instructions. The phosphorylated RTKs were detected with the ECL system, and the densitometric values of duplicate spots were normalized using several positive controls spotted on the two diametrically opposite corners of the membrane, which were then quantified using the Cell Profiler Software. The values after normalization represent the mean of duplicate spots for each protein.

Statistical analysis. All statistical analyses were performed using the SPSS 21.0 System. Two independent samples were compared using the student t test. Multiple pairwise comparisons were made using a one-way analysis of variance (ANOVA). A $P<0.05$ was considered to be statistically significant.

Results

Rigosertib is selectively toxic against MDS and leukemia cells. Rigosertib induced increased apoptosis in CD34+ cells from MDS patients, especially from high-grade MDS patients, in a dose-dependent manner (Figure 1A). Similarly, rigosertib also increased apoptosis in MDS/leukemia cell lines, including MDS-L, SKM1, U937, K562, Kasumi-1 and KG1a (Figure 1B). However, rigosertib could not induce apoptosis in CD34+ cells from normal controls (Figure 1C). To assess the LD50, CD34+ cells and cell lines were exposed to increasing concentrations of rigosertib ranging from 0.5 μmol/L to 20 μmol/L for 24 hours. The LD50 value was obtained by calculating the percentage of CD34+ cells stained with Annexin V (including positive Annexin V alone and both positive Annexin V and PI) in each sample at 24 hours. As shown in Table 1, the LD50 values in MDS patients and cell lines ranged from 5.6 to 28.1 μmol/L and from 6.1 to 13.2 μmol/L, respectively, while those of normal controls usually exceeded 50 μmol/L. In addition, the LD50 values of patients with high-grade MDS were lower than those of patients low-grade MDS (Figure 1D). In summary, rigosertib showed selective cytotoxcity against MDS and MDS/leukemia cell lines but not against normal cells.

Rigosertib induces apoptosis of CD34+ cells with relapsed MDS who previously responded to decitabine treatment. Rigosertib was

Table 1 | Clinical characteristics of MDS patients and expression of signal pathway protein in MDS CD34+ cells

No.	Sex	Age	Diagnosis*	IPSS-R	Karyotype	Rigosertib, ([&]LD50, 24 h, μmol/L)	#Relative expression (fold change, MDS/Normal controls)									
							Akt1	*p-Akt1*	*p-p38*	*p-ERK1/2*	*p-JNK*	*p-STAT1*	*p-STAT3*	*p-β-catenin*	*p-GSK 3α/β*	*p-p53*
P1	M	76	RARS	4.5	Del(11q)	25.6	0.91	0.91	2.14	2.33	3.10	0.54	1.19	0.91	1.61	1.76
P2	M	56	MDS-U	1.5	Normal	NA*	1.23	0.77	2.50	2.00	3.53	0.89	1.40	0.96	0.91	1.88
P3	F	62	RCMD	2.5	Normal	18.5	0.84	1.15	1.50	2.01	1.29	NA	0.81	NA	NA	NA
P4	M	45	RCMD	5	Trisomy 8	NA	1.35	1.49	2.07	1.57	3.02	1.25	0.97	1.68	1.71	0.99
P5	F	40	RCMD	2	Normal	NA	0.76	0.58	1.00	1.12	3.10	2.32	0.65	1.01	2.32	1.65
P6	M	81	RCMD	6	Trisomy 8	NA	1.93	1.78	1.29	1.19	2.16	1.79	2.21	2.21	2.52	1.10
P7	M	60	RCMD	6	t(5;11), del(17p)	NA	1.66	1.78	1.79	0.84	2.59	1.61	1.94	1.83	2.21	1.32
P8	M	29	RCMD	4	Trisomy 8	NA	1.05	1.34	2.14	0.60	2.41	1.52	1.08	1.11	1.51	1.43
P9	M	57	RCMD	3	Del(7q)	NA	1.10	0.91	1.43	2.58	2.41	1.34	0.81	0.77	0.40	0.77
P10	F	58	RCMD	3.5	Trisomy 8	14.2	1.53	2.06	2.36	0.77	3.45	0.71	0.70	1.54	1.21	1.54
P11	M	52	RCMD	7	5q-,-7,-13,-18	NA	2.47	2.21	1.14	0.87	1.81	0.54	1.67	1.63	1.91	1.43
P12	M	72	RCMD	3.5	Normal	NA	0.85	1.49	2.86	1.35	4.14	0.80	1.40	1.30	1.01	1.21
P13	M	78	RCMD	5	del(5q), inv(9)	NA	2.12	1.97	1.71	2.92	1.03	1.07	1.57	0.87	0.81	1.32
P14	M	79	RCMD	5	-5,-16,-18,-20	8.6	2.26	1.63	1.79	0.58	0.78	NA	2.05	1.97	0.70	0.88
P15	F	53	RCMD	4	Normal	28.1	0.87	1.25	1.86	0.97	NA	0.45	NA	1.44	0.50	2.21
P16	F	64	RCMD	4.5	-X, tri3, t(7;11)	7.4	1.66	2.40	1.79	0.77	0.60	1.16	0.27	1.20	1.21	0.88
P17	M	53	RCMD	4.5	Normal	10.7	2.08	2.16	0.93	0.87	NA	0.45	NA	1.73	NA	NA
P18	M	60	RAEB-1	4	Normal	10.4	2.05	2.16	1.50	2.28	1.90	0.71	2.27	1.11	2.01	0.47
P19	F	64	RAEB-1	7.5	-7	NA	2.57	3.31	1.14	0.87	1.38	0.80	2.10	1.59	1.71	0.65
P20	F	62	RAEB-1	6	Del(9q),Del(20q)	NA	3.16	3.55	2.29	1.26	2.67	0.89	0.65	0.96	2.32	0.54
P21	M	68	RAEB-1	8.5	-3, del(5q), -6	7.1	2.33	2.69	1.64	1.16	0.69	1.61	2.21	1.63	1.41	0.76
P22	M	70	RAEB-1	4.5	Trisomy 8	NA	1.62	2.21	2.21	1.06	1.38	1.43	3.45	1.78	1.71	0.55
P23	F	59	RAEB-1	5	Normal	NA	2.94	2.45	1.29	1.83	2.07	1.34	1.89	1.68	3.52	0.44
P24	M	61	RAEB-1	4.5	Normal	NA	1.72	1.82	3.00	1.35	1.21	0.71	1.08	1.49	2.11	1.10
P26	F	40	RAEB-1	6	Trisomy 8	NA	2.04	1.68	1.79	1.16	1.38	1.43	1.13	1.35	2.82	1.54
P25	M	68	RAEB-2	9	Der(3;5), -6, tri8	NA	2.28	2.97	0.79	0.97	1.64	1.07	2.43	1.73	3.02	0.89
P27	F	50	RAEB-2	5.5	normal	12.6	1.56	2.25	1.79	2.43	NA	0.71	0.65	1.63	0.50	0.99
P28	F	39	RAEB-2	5.5	Normal	7.5	2.71	2.59	1.21	0.58	2.59	0.98	1.78	1.83	2.42	0.75
P29	F	64	RAEB-2	5.5	Normal	NA	3.24	3.12	2.14	3.44	2.50	1.16	1.94	1.54	3.22	1.21
P30	M	50	RAEB-2	4	Normal	5.6	2.36	2.30	1.29	1.57	NA	1.61	1.89	1.68	2.52	0.86
P31	F	61	RAEB-2	6	Del(5q)	10.2	2.11	2.25	0.71	0.58	1.38	1.79	1.35	1.49	3.12	0.73
P32	F	70	RAEB-2	5.5	Normal	8.6	2.48	2.59	0.36	2.93	1.38	1.96	1.19	1.30	0.81	1.32
P33	F	34	RAEB-2	7.5	Trisomy 8	6.4	1.79	1.78	0.64	0.77	NA	1.34	1.51	2.16	1.31	0.63
P34	M	47	RAEB-2	6	Normal	8.2	3.12	2.78	1.07	0.39	1.90	1.07	2.05	1.92	3.22	0.76
P35	M	62	RAEB-2	5.5	Normal	NA	2.65	2.49	1.43	0.48	2.67	1.52	2.00	0.87	1.71	0.97

*Morphologic diagnosis at presentation in MDS according to WHO classification. RA, refractory anemia; RCMD, refractory cytopenia with multilineage dysplasia; RAEB-1/2, refractory anemia with excess blasts 1/2.
F, female; M, male. IPSS-R, revised international prognostic scoring system. NA, not available.
[&]In order to assess the LD50, CD34+ cells and cell lines were exposed to increasing concentrations of rigosertib ranging from 0.5 μmol/L to 20 μmol/L for 24 hours. The LD50 value was obtained by calculating the percentage of CD34+ cells stained with Annexin V in each sample at 24 hours
#The expression or phosphorylation of signal pathway proteins in CD34+ cells was quantified by flow cytometry based on the mean fluorescence intensity (MFI). The relative expression was represented in the ratio of MFI (MDS: Normal control). p-Akt1, phosphorylated Akt1.

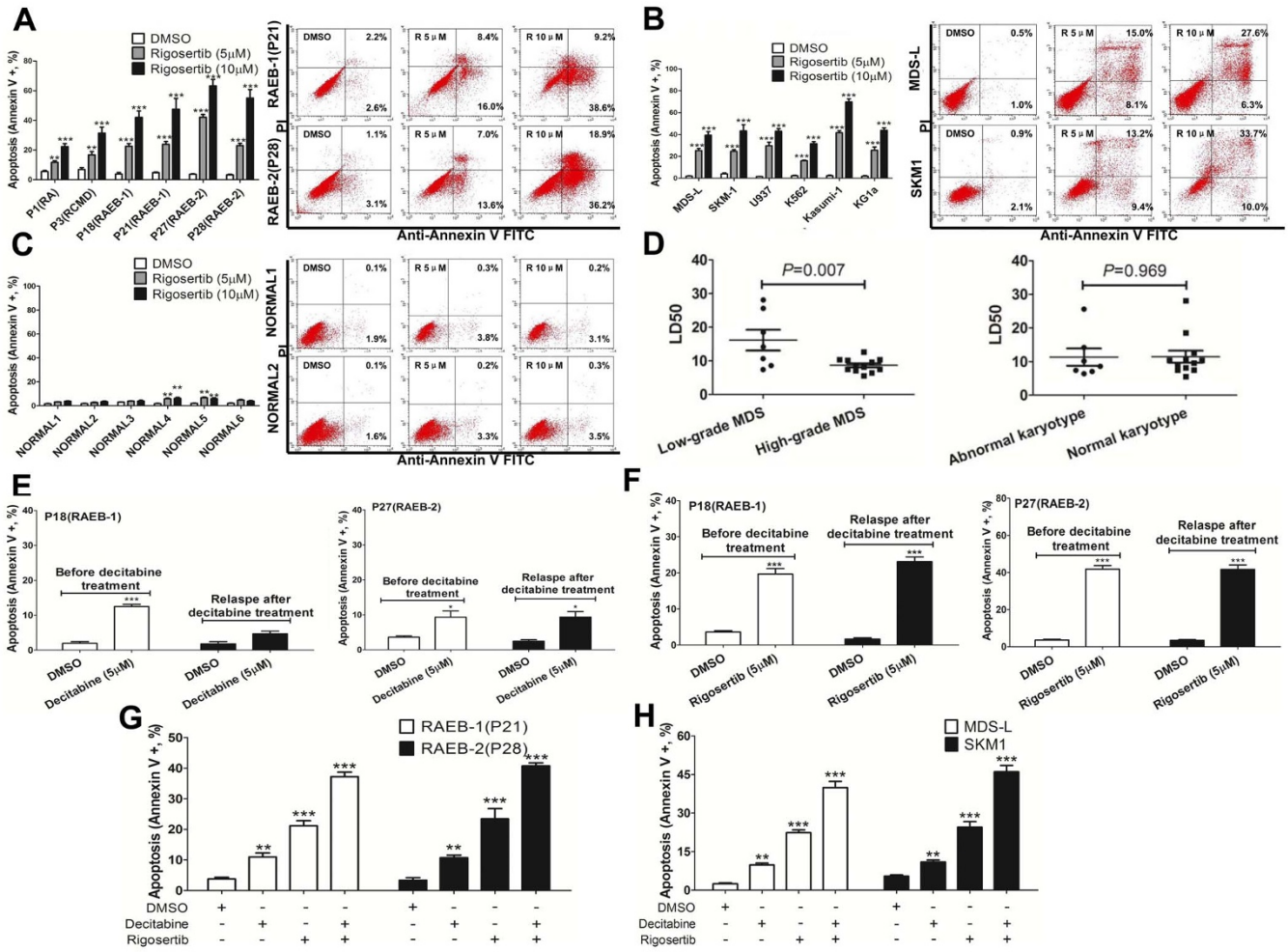

Figure 1 | Induction of apoptosis by Rigosertib in MDS patients, normal controls and cell lines. (A) Rigosertib induced increased apoptosis in CD34+ cells from MDS patients. Especially those from high-grade MDS (Left), in a dose-dependent manner (Right); (B) rigosertib also induced increased apoptosis in MDS and leukemia cell lines, including MDS-L, SKM1, U937, K562, Kasumi-1 and KG1a (Left), in a dose-dependent manner (Right); (C) rigosertib could not induce apoptosis in CD34+ cells from normal controls; (D) the LD50 values were lower in patients with high-grade MDS than in those with low-grade MDS (left). Patients with a normal and abnormal karyotype did not differ; (E) decitabine (5 μM) induced apoptosis in CD34+ cells from RAEB-1 (Left) and RAEB-2 (Right) in vitro before decitabine treatment. However, decitabine did not induce significant apoptosis in CD34+ cells from relapsed RAEB-1 (Left) in vitro that previously responded to decitabine treatment; (F) decitabine (5 μM) strongly induced apoptosis in CD34+ cells from RAEB-1 (Left) and RAEB-2 (Right) in vitro obtained before decitabine treatment or after disease relapse; (G) and (H) rigosertib combined with decitabine could synergistically induce cell apoptosis in MDS CD34+ cells and cell lines. For RAEB-1 or RAEB-2 such Figure G, the results included those from two RAEB-1 patients (P18 and P21) and two RAEB-2 patients (P27 and P28). Error bars throughout represent the SEM. For each patient or cell line, experiments were carried out three times. Corresponding statistical analysis relative to control is annotated by an asterisk. *, $P<0.05$; **, $P<0.01$; ***, $P<0.001$ (two-tailed, student T test).

used to treat higher risk MDS following hypomethylating treatment in several clinical trials[11–13]. Thus, we primarily investigated the cytotoxic effect of rigosertib on the CD34+ cells from relapsed MDS that previously responded to decitabine treatment. These relapsed patients failed to respond to decitabine treatment again despite previously achieving a treatment response. Four samples with CD34+ cells from two patients (1 RAEB-1 and 1 RAEB-2) were co-incubated with decitabine or rigosertib before clinical decitabine treatment and after relapse (Figure 1E and 1F). Both decitabine (5 μM) and rigosertib (5 μM) induced cell apoptosis in vitro before clinical decitabine treatment. Interestingly, rigosertib still induced apparent cell apoptosis in CD34+ cells from relapsed patients. However, decitabine could not induce cell apoptosis in CD34+ cells from one of the two relapsed patients. Rigosertib was more cytotoxic than decitabine against MDS primary CD34+ cells both before decitabine therapy and after relapse when administered at the same concentration as decitabine. Moreover, rigosertib combined with decitabine could induce synergistic cell apoptosis in CD34+ cells with MDS and cell lines (Figure 1G and 1H).

Rigosertib induces cell cycle arrest into G2/M and inhibited proliferation of MDS cells. Rigosertib slightly induces G2/M phase block and decreased the percentage of MDS CD34+ cells in the S phase compared to the control cells (Figure 2A). Rigosertib also induced significant G2/M phase block and decreased the percentage of cells in S phase in MDS/leukemia cell lines (Figure 2B). However, rigosertib did not induce cell cycle arrest at the G2/M phase in normal CD34+ cells, as evidenced by almost all of these cells transitioning to the G0/G1 phase (Figure 2C). Low dose of rigosertib (0.5 μM) inhibited the proliferation of MDS CD34+ cells in a time-dependent and dose-dependent manner (Figure 2D). The proliferation of MDS cell lines was also apparently inhibited in a time-dependent and dose-dependent manner (Figure 2E).

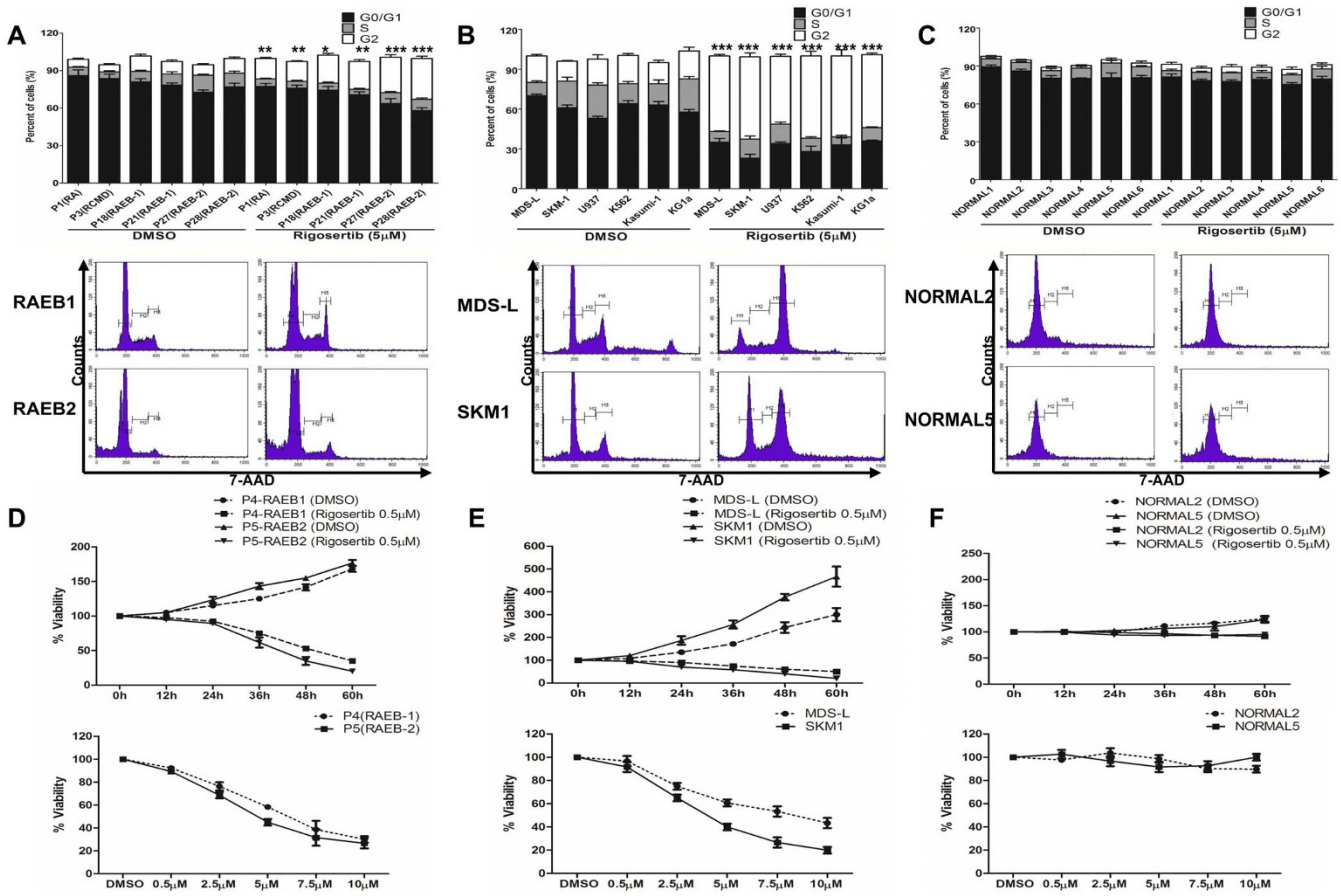

Figure 2 | Rigosertib induces cell cycle arrest into G2/M and inhibited proliferation of MDS cells. (A) Rigosertib resulted in moderate G2/M arrest in CD34+ cells from MDS patients (up). The representative graphs for two patients (RAEB-1 and RAEB-2) are shown (down); (B) rigosertib could induce significant G2/M phase block and decrease the percentage of cells in the S phase in the MDS and leukemia cell lines. The representative graphs for MDS-L and SKM1 cell lines are shown (down); (C) rigosertib could not induce cell cycle arrest at the G2/M phase in normal CD34+ cells. The representative graphs are shown (down); (D) A low dose of rigosertib (0.5 μM) inhibited the proliferation of MDS CD34+ cells in a time-dependent (top) and dose-dependent manner (down) with the support of stem cell growth factors; (E) The proliferation of MDS-L and SKM1 cells was also apparently inhibited with a time-dependent (top) and dose- dependent manner (top); (F) Rigosertib minimally affected the proliferation of normal CD34+ cells. Error bars throughout represent the SEM. *, $P<0.05$; **, $P<0.01$; ***, $P<0.001$ (two-tailed, student T test).

Rigosertib minimally affected the proliferation of normal CD34+ cells (Figure 2F).

Rigosertib activates the P53-mediated mitochondrial cell death and cell cycle arrest.. As described above, rigosertib induced cell apoptosis and cycle arrest in the G2/M phase. To investigate the mechanism of action of rigosertib in apoptosis and the cell cycle, MDS cell lines, primary MDS and normal CD34+ cells were treated with 5 μmol/L rigosertib for 12 hours. First, the mitochondrial membrane potential was analyzed by detecting mitochondrial depolarization. Compared with the DMSO control, rigosertib decreased the mitochondrial potentials and produced obvious monomers in primary MDS CD34+ cells (Figure 3A). Similarly, rigosertib also markedly decreased the mitochondrial potentials in MDS and leukemia cell lines (Figure 3B). Conversely, rigosertib had little impact on the mitochondrial potentials of normal CD34+ cells (Figure 3C).

Next we further investigated the effect of rigosertib on the P53-mediated mitochondrial death pathway and cell cycle control. The levels of pathway-associated pro-apoptotic proteins, including P21, bax, active PARP, active caspase-3, were determined via FCM. Rigosertib markedly elevated the expression of pathway-associated apoptosis proteins in MDS CD34+ cells and cell lines (Figure 3D and 3E). In contrast, rigosertib did not increase the level of these apoptosis proteins in normal CD34+ cells (Figure 3F). The levels of anti-apoptosis and cycle control proteins, such as bcl-2, Cyclin B1 and Cyclin D1, were also evaluated by FCM. The results showed that rigosertib inhibited the expression of bcl-2 and Cyclin D1 in primary MDS CD34+ cells and MDS cell lines while having no effect in normal CD34+ cells (Figure 3G, 3H and 3I). To further confirm these results, these pathway-associated proteins were validated using a western blot assay in MDS cell lines. The same results were observed in the western blot assay (Figure 3J). In addition, rigosertib increased the level of CDK1 and Cyclin B1 but decreased CDC25C phosphorylation in MDS cell lines (Figure 3J). CDK1, Cyclin B1 and CDC25C are considered to take part in P53-dependent cell cycle arrest at the G2/M phase[19,20]. Taken together, these results revealed that rigosertib activates the P53-mediated mitochondrial cell death pathway and cell cycle arrest in G2/M.

Identification of multiple dysregulated signaling transduction pathways by GEM and bioinformatics analysis. Because rigosertib was applied as a kinase inhibitor in clinical trials, the possible dysregulation of signaling transduction pathways in MDS merits investigation. The GEM analysis from CD34+ cells of 12 MDS patients showed 1783 differentially expressed genes compared with the results from 6 normal controls: 405 were upregulated, while 1378 genes were downregulated. 302 of the 1783 genes

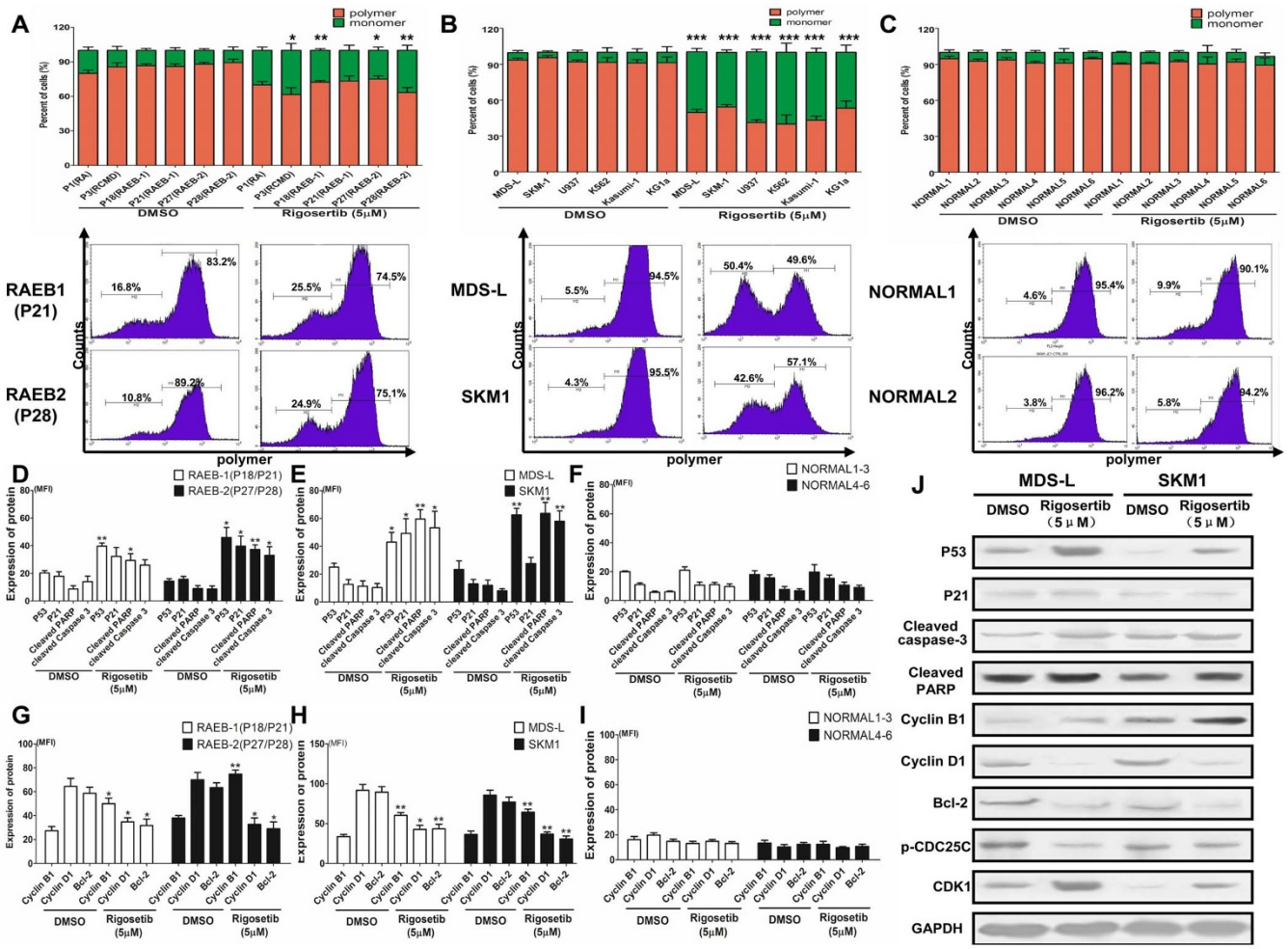

Figure 3 | Rigosertib activates the P53-mediated mitochondrial cell death and cycle pathway. (A) Rigosertib reduced the mitochondrial potentials and produced obvious monomers in MDS CD34+ cells. The representative graphs are shown (down); (B) rigosertib also markedly decreased the mitochondrial potentials in MDS and leukemia cell lines. The representative graphs are shown (down); (C) rigosertib had little impact on the mitochondrial potentials in normal CD34+ cells. The representative graphics are shown (down); Rigosertib markedly increased the expression of P53 pathway-associated apoptosis proteins, such as P53, P21, cleaved PARP and cleaved caspase 3 in primary MDS CD34+ cells (D) and MDS cell lines (E); (F) rigosertib could not increase the level of these apoptosis proteins in normal CD34+ cells; (G) and (H) rigosertib inhibited the expression of the anti-apoptosis proteins bcl-2 and Cyclin D1 in MDS CD34+ cells and cell lines; (I) Rigosertib did not affect these anti-apoptosis proteins in normal CD34+ cells; (J) These P53 pathway-associated proteins were validated via western blot in MDS and leukemia cell lines. The same results were observed for the western blot assay. In addition, rigosertib increased the levels of CDK1 and Cyclin B1 but decreased CDC25C phosphorylation, which may be responsible for G2/M arrest. For each patient or cell line, experiments were carried out three times. For RAEB-1 or RAEB-2 such Figure G, the results included those from two RAEB-1 patients (P18 and P21) and two RAEB-2 patients (P27 and P28). Error bars throughout represent the SEM. *, $P<0.05$; **, $P<0.01$; ***, $P<0.001$ (two-tailed, student T test).

may regulate or be regulated by 175 signaling pathways. Hierarchical clustering showed that the Akt-PI3K, MAPK, Jak-STAT, Wnt, Adipocytokine, Notch and P53 signaling pathways encompassed 28, 16, 17, 8, 5,5 and 5 differentially expressed genes, respectively (Figure 4A-4G). Next, pathway analysis showed that 31 significant pathways were affected by upregulated genes and 14 were significantly affected by downregulated genes in MDS patients (the first 5 pathways were shown in Figure 4H): the Akt-PI3K, MAPK, Jak-STAT, Wnt and Notch signaling pathways were considered the most significant pathways that are primarily dysregulated in MDS patients. Further pathway-net analysis revealed that the MAPK, Jak-STAT and apoptosis signaling pathways were described as key downstream pathways, through which other signaling pathways may perform their biological function in MDS (Figure 4I). A previous report suggested that MAPK signaling was dysregulated in MDS and associated with over-activated cell apoptosis[21]. Taken together, a combination of GEM and bioinformatics analysis identified a series of dysregulated pathways that may ultimately point to the regulation of apoptotic cell death.

Phosphorylation level of key signaling transducers from dysregulated pathways was validated by FCM in MDS patients. To validate the dysregulated signaling pathways identified by GEM and bioinformatics analysis, we employed FCM to determine the expression and phosphorylation level of key proteins from these pathways in MDS primary CD34+ cells. A total of 13 normal controls and 35 MDS patients were involved in the FCM analysis. The MDS cases consisted of 17 low-grade (1 RARS, 1 MDS-U, 15 RCMD) and 18 high-grade (8 RAEB-1, 10 RAEB-2) patients according to the WHO classification. Usually, a signaling pathway contains many proteins, including transmembrane receptors, intracellular mediators, transcription factors and target genes, which may not be individually analyzed. However, the phosphorylation of intracellular mediators at specific amino acid residues was consi-

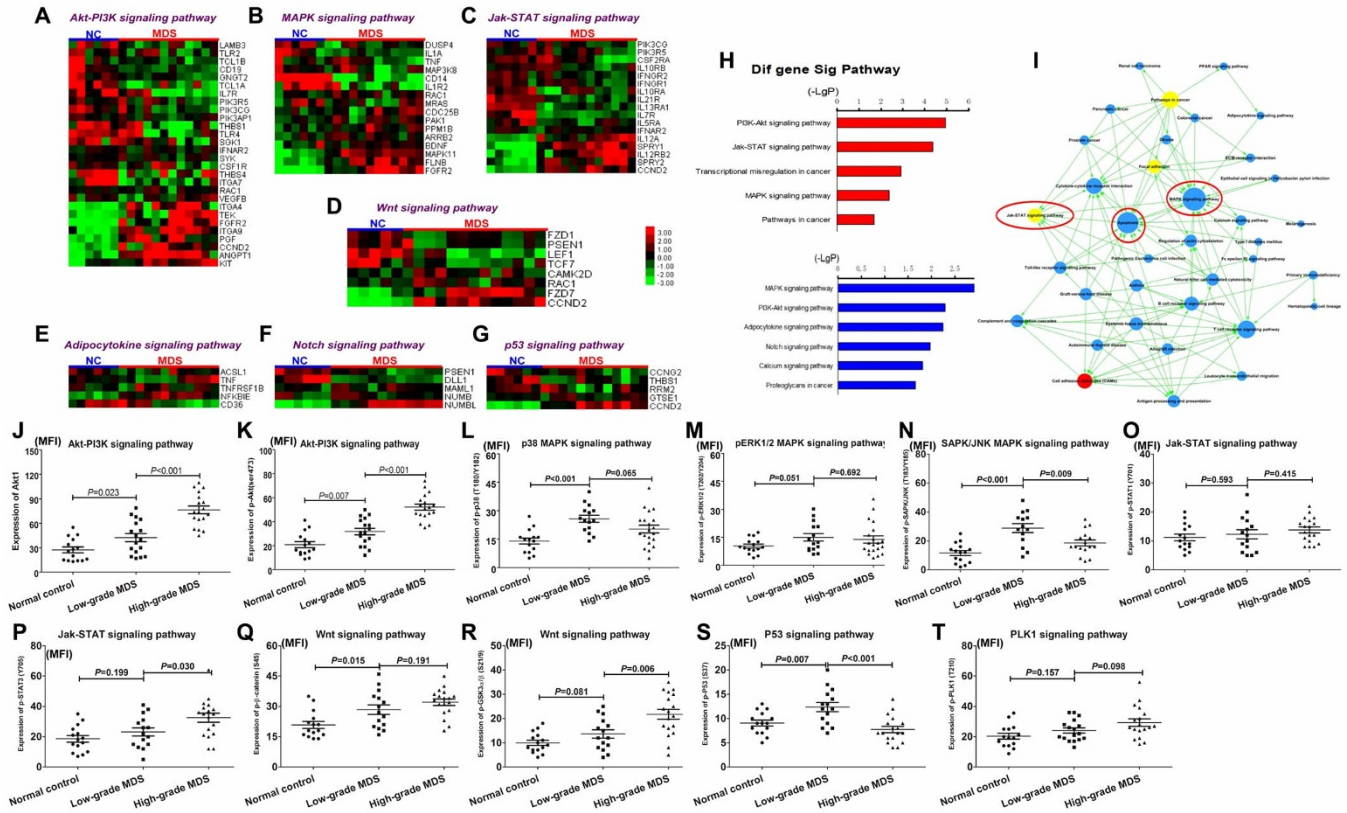

Figure 4 | Identification of multiple dysregulated signaling transduction pathways by GEM and FCM. The Akt-PI3K (A), MAPK (B), Jak-STAT (C), Wnt (D), Adipocytokine (E), Notch (F) and P53 (G) signaling pathways were identified with hierarchical clustering as potentially significant pathways that may be dysregulated in MDS (n=12) compared with normal controls (NC; n=6); (H) Further pathway analysis showed that the Akt-PI3K, MAPK, Jak-STAT, Wnt and Notch signaling pathways were considered remarkably significant; (I) pathway-net analysis revealed that the MAPK, Jak-STAT and apoptosis signaling pathways were described as key downstream pathways; (J) and (K) Akt1 and Akt phosphorylation in Akt-PI3K pathway were evidently elevated in MDS (n=35) patients compared to the normal controls (n=15). High-grade MDS (n=18) exhibited higher expression levels of Akt1 and Akt phosphorylation; (L) the p38 phosphorylation in the p38 MAPK pathway was higher in MDS patients, especially in low-grade MDS, than in normal controls; (M) and (N) no significant difference in the phosphorylated ERK1/2 (ERK MAPK pathway) and SAPK/JNK (JNK MAPK pathway) levels was observed between the MDS and normal group; (O) no difference in phosphorylated STAT1 was observed in the Jak-STAT pathway between the MDS and normal group; (P) MDS patients showed increased STAT3 phosphorylation in the Jak-STAT pathway in the MDS group, especially high-grade patients. (Q) and (R) the levels of phosphorylated GSK-3α/β (Ser9) and β-catenin (Ser45) were significantly increased in MDS patients compared to the normal controls. In addition, the P53 signaling pathway was also investigated due to its critical role in regulating cell apoptosis in MDS; (S) P53 phosphorylation was significantly increased in low-grade MDS compared to normal controls and high-grade MDS; (T) the level of PLK1 phosphorylation did not differ between MDS and normal controls. Error bars throughout represent the SEM. The comparison analysis among normal controls, low-grade and high-grade MDS groups were performed using ANOVA test.

dered a marker of the activation of signaling pathways. Therefore, we evaluated the dysregulated pathways identified by GEM by determining the phosphorylation level of key signaling transducers in pathways. For the Akt-PI3K signaling pathway, the Akt1 expression and phosphorylation levels of Akt at Ser473 were evidently elevated in MDS patients compared to normal controls (Figure 4J and 4K). High-grade MDS exhibited higher expression levels of Akt1 and Akt phosphorylation. In the MAPK signaling pathway, which consists of p38, ERK1/2 and SAPK/JNK, p38 phosphorylation at Thr180/Tyr182 was higher in MDS patients, especially in low-grade MDS, than that in normal controls (Figure 4L). The levels of phosphorylated ERK1/2 (Thr202/Tyr204) and SAPK/JNK (Thr183/Tyr185) did not significantly differ between the MDS and normal group (Figure 4M and 4N). For the Jak-STAT signaling pathway, MDS patients showed increased STAT3 phosphorylation at Tyr705 in the MDS group, especially high-grade patients, while the levels of phosphorylated STAT1 at Tyr701 did not differ between the MDS and normal group (Figure 4O and 4P). For the Wnt signaling pathway, the levels of phosphorylated GSK-3α/β (Ser9) and β-catenin (Ser45) were significantly increased in MDS patients compared to the normal controls (Figure 4Q and 4R). The P53 signaling pathway was also investigated due to its critical role in regulating cell apoptosis in MDS. P53 phosphorylation was significantly increased in low-grade MDS compared the normal controls and high-grade MDS (Figure 4S). In addition, no significant difference was observed between MDS and normal controls groups (Figure 4T).

Rigosertib could modify multiple signaling pathways in MDS CD34+ cells and cell lines. To further access the effect of rigosertib on the dysregulated signaling pathways in MDS, MDS CD34+ cells, cell lines and normal CD34+ cells were treated with 5 μmol/L of rigosertib in vitro. After 12 hours, the cells were collected, and the signaling transducers were detected by FCM and western blot. The phosphorylated signaling transducers identified via GEM and bioinformatics analysis in MDS, such as Akt, p38, SAPK/JNK, STAT3, β-catenin, GSK3α/β and P53 as well as PLK1, were included into this assay. As shown in Figure 5A, rigosertib did not affect the expression or phosphorylation levels of signaling transducers in normal CD34+ cells because of non-activation of

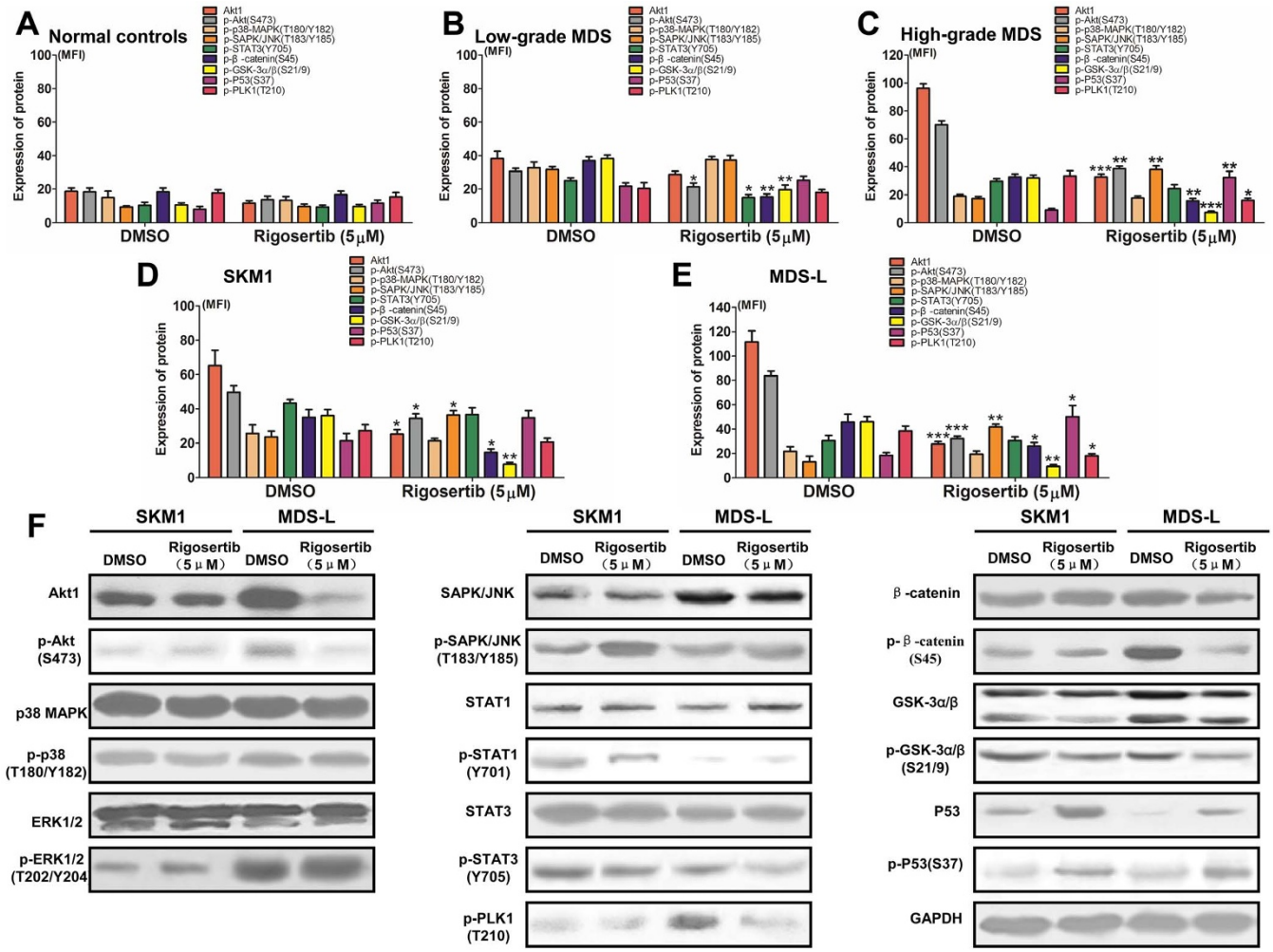

Figure 5 | Rigosertib could modify multiple signaling pathways in MDS and MDS cell lines. (A) Rigosertib did not affect the expression and phosphorylation levels of signaling transducers, including Akt, p38, SAPK/JNK, STAT3, β-catenin, GSK3α/β and P53, in normal CD34+ cells because it did not activate these proteins; (B) In patients with low-grade MDS, rigosertib administration could somewhat reduce the phosphorylation of Akt, β-catenin and GSK3α/β; (C) In patients with high-grade MDS, rigosertib markedly reduced the phosphorylation of Akt, β-catenin and GSK3α/β, while the phosphorylation of SAPK/JNK and P53 was enhanced; In the SKM1 (D) and MDS-L (E) cell lines, the same results could be observed as in patients with high-grade MDS. (F) Western blot was performed to validate the results acquired from FCM in the MDS-L and SKM1 cell lines. Representative graphic from three experiments was shown. For each patient or cell line, experiments were carried out three times. Error bars throughout represent the SEM. *, $P<0.05$; **, $P<0.01$; ***, $P<0.001$ (two-tailed, student T test).

these proteins. In patients with low-grade MDS, rigosertib administration could somewhat reduce the phosphorylation of Akt, β-catenin and GSK3α/β (Figure 5B). In patients with high-grade MDS, rigosertib markedly reduced the phosphorylation levels of Akt, β-catenin and GSK3α/β, while the phosphorylation levels of SAPK/JNK and P53 were enhanced (Figure 5C). Similar results could be observed in the MDS-L and SKM1 cell lines (Figure 5D and 5E). Moreover, western blot was performed to validate the results acquired from FCM in the MDS-L and SKM1 cell lines. Apparently, rigosertib could diminish the phosphorylation levels of Akt, STAT3, β-catenin and GSK3α/β, whereas it reinforced the phosphorylation levels of SAPK/JNK and P53 (representative graphics shown in Figure 5F). Rigosertib could meliorate these dysregulated pathways by inhibiting anti-apoptosis-related pathways and activating apoptosis-related pathways in MDS, especially in high-grade MDS.

Identification of rigosertib-targeted RTKs by RTK phosphorylation array. Because RTKs bind and activate intracellular signaling transducers, we further attempted to identify the RTKs that were targeted by rigosertib. The MDS and SKM1 cell lines were tested with a phosphorylation antibody array specifically designed to simultaneously identify the relative levels of phosphorylation of 71 different human RTKs. In the MDS-L cell line, rigosertib increased the phosphorylation levels of FRK, Fyn, LCK, RET, PDGFR-β and TNK1 but decreased the phosphorylation levels of Tie2, ZAP70, FGFR2, Tyk2 and VEGFR2 (the fold change >2) (Figure 6A and 6B). In the SKM1 cell line, rigosertib increased the phosphorylation levels of PDGFR-β, Blk, EphA1, ErbB2, PYK2, RET and SYK but decreased the phosphorylation levels of Tie2, VEGFR2 and RYK (the fold change >2) (Figure 6C and 6D). Two up-regulated RTKs (RET and PDGFR-β) and two down-regulated RTKs (Tie2 and VEGFR2) were shared as rigosertib-targeted RTKs in the MDS-L and SKM1 cell lines. The interaction of RTKs with intracellular signaling transducer-targeted rigosertib should be further investigated to elucidate the precise mechanisms of rigosertib in this specific pathway.

Discussion

Rigosertib is a member of a broader class of unsaturated sulfone kinase inhibitors that allosterically inhibit substrate binding[13,22]. Rigosertib has received increasing focus due to its promising anti-tumor activity in a wide variety of cancer cells without affecting the proliferation and survival of normal cells. Given the high anti-tumor

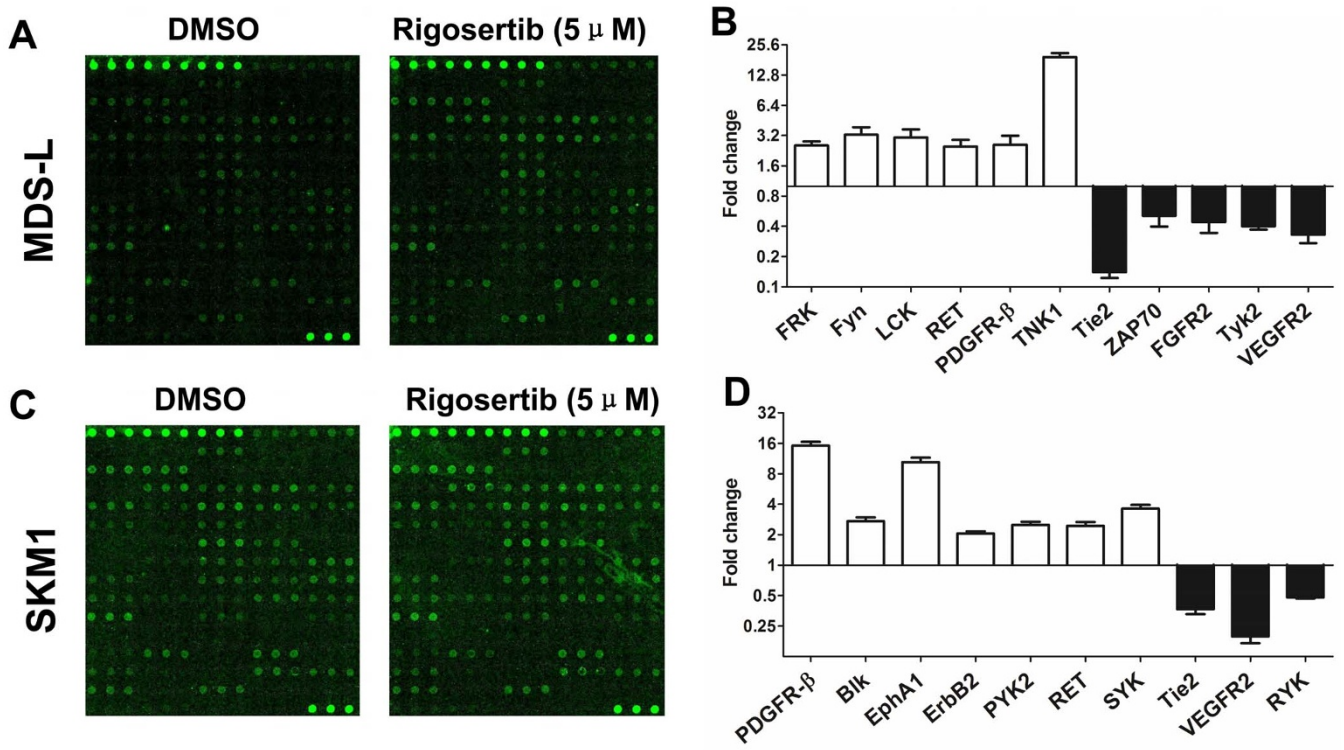

Figure 6 | Identification of rigosertib-targeted RTKs. (A) and (B) rigosertib increased the phosphorylation levels of FRK, Fyn, LCK, RET, PDGFR-β and TNK1 but decreased the phosphorylation levels of Tie2, ZAP70, FGFR2, Tyk2 and VEGFR2 (the fold change > 2) in the MDS-L cell line; (C) and (D) rigosertib increased the phosphorylation levels of PDGFR-β, Blk, EphA1, ErbB2, PYK2, RET and SYK but decreased the phosphorylation levels of Tie2, VEGFR2 and RYK (the fold change > 2) in the SKM1 cell line. Error bars throughout represent the SEM.

activity and low toxicity of rigosertib, a multinational pivotal phase 3 randomized clinical trial of rigosertib versus the best supportive care for patients with high-grade MDS following prior treatment with hypomethylating agents is ongoing[13]. In this situation, exploring the mechanism of action of rigosertib in MDS is indispensable to prevent unexpected outcomes due to clinical administration ahead of basic study, such as frequent resistance during hypomethylation treatment. In this study, we attempted to obtain more information about the effect of rigosertib on multiple signaling pathways in MDS via a series of experiments.

The effect of rigosertib on tumor biology in MDS was first investigated. The cytotoxic experiments in vitro revealed that apoptosis was selectively induced in MDS primary CD34+ cells and MDS/leukemia cell lines, while normal CD34+ cells were not or only minimally affected. This strong ability to induce apoptosis in MDS was unexpected. In primary CD34+ cells from patients receiving decitabine treatment, rigosertib induced much stronger apoptosis in vitro than decitabine, both in cells obtained prior to decitabine treatment and after disease relapse. The strong pro-apoptotic ability and concurrent minimal effects on normal cells may justify a pivotal phase 3 randomized clinical trial. In addition, the synergistic effect of rigosertib with decitabine suggested that the combination of both agents may be considered as a candidate strategy in clinical practice. Rigosertib also induced cell cycle arrest at the G2/M phase and inhibited the proliferation of MDS primary CD34+ cells and cell lines, which was consistent with previous reports in solid tumors[5–7]. Further mechanistic studies showed that the activation of cyclin B1-associated CDK1 may be responsible for G2/M arrest. Rigosertib induced apoptosis by enhancing the P53-mediated mitochondrial apoptosis pathway. In a phase I study of advanced solid tumors, inactivated p53 was suggested to predict the treatment response to rigosertib[10]. P53 inactivation was frequent in high-grade MDS[23,24], which may also be considered another crucial basis for rigosertib treatment.

Increasing evidence indicates that MDS cells harbor multiple genetic and epigenetic abnormalities[25,26]. Numerous mutational genes participating in transcription regulation and epigenetic modification in MDS have been identified, such as SF3B1, SRSF2, TET2, ASXL1, EZH2, DNMT3A, etc[25]. The functional integration of the above mutations may drive an imbalance between apoptosis- and proliferation-related signaling transduction pathways. In this study, a combination of GEM and bioinformatics utilities was used to comprehensively analyze the differentially expressed genes around a specific signaling pathway to indirectly identify various dysregulated pathways. Further validation analysis by FCM revealed the abnormal activation of the p38 MAPK, SAPK/JNK and P53 pathways in low-grade MDS, while the Akt-PI3K, Jak-STAT and Wnt pathways were activated in high-grade MDS. Our study for the first time provides an overview of multiple dysregulated signaling transduction pathways based on GEM and bioinformatics analysis. Previous studies exhibited that the excessive activation of apoptosis- and proliferation-related signaling pathways in low-grade and high-grade MDS, respectively. The excessive activation of the p38 MAPK and TGF-β signaling pathways promoted the aberrant apoptosis of hematopoietic stem and progenitor cells in low-grade MDS, while the Akt-PI3K, PI3K-mTOR and EGF signaling pathways were over-activated in high-grade MDS[27–30]. The corresponding inhibitors have been applied to treat low-grade and high-grade MDS in several phase I/II clinical trials and showed moderate treatment responses, and most of these agents failed to enter phase III clinical trials due to unsatisfactory responses and severe toxicity. The multiple dysregulated signaling transduction pathways in MDS prompted us to select multiple-kinase inhibitors in clinical trials to overcome disease heterogeneity and maximize the therapeutic effect. Therefore, rigosertib

was selected and has shown promise in several I/II clinical trials with MDS as a dual-kinase inhibitor of the Polo-like kinase and Akt/PI3 kinase pathways[11–13].

As mentioned above, rigosertib could inhibit the Akt-PI3K and PLK1 signaling pathways. Akt activation was frequently observed, while PLK activation was rare in MDS patients. In addition, LY294002 as a sole Akt-PI3K inhibitor could not induce obvious cell apoptosis in MDS[29]. Thus, rigosertib may have additional effects because it is a multi-kinase inhibitor. Moreover, the LD50 values are lower in high-grade MDS than in low-grade MDS, indicating that the abnormal biological signaling targeted by rigosertib mainly occurred in high-grade MDS. Further in vitro experiments support this finding. In addition to Akt-PI3K, rigosertib could markedly inhibit the activation of the Jak-STAT and Wnt signaling pathways; furthermore, rigosertib activated the SAPK/JNK and P53 signaling pathways. These findings suggest that rigosertib is more than a simple dual-kinase inhibitor. Moreover, an RTK phosphorylation array showed that rigosertib also modulated the activity of several RTKs. Some RTKs, such as Tie2 and VEGFR2, usually bind and phosphorylate Akt-PI3K or ERK1/2 when activated to subsequently activate these pathways[31,32]. Hence, rigosertib exerts dual functions in intracellular signaling pathways and membrane RTKs. These data greatly enriched our understanding of the mechanism of action of rigosertib and provided more experimental information for clinical administration.

Our results showed that rigosertib is a selective and promising anti-tumor agent that induces apoptosis and G2/M arrest via activation of the P53-mediated mitochondrial pathway. Moreover, new insights were provided into the mechanism of action of rigosertib, which showed that this agent acted as a multi-kinase inhibitor to meliorate multiple dysregulated signaling transduction pathways in high-grade MDS.

1. Li, X., Bryant, C. E. & Deeg, H. J. Simultaneous demonstration of clonal chromosome abnormalities and apoptosis in individual marrow cells in myelodysplastic syndrome. *Int J Hematol* **80**, 140–1405 (2004).
2. Li, X, Song, Q. & Chen, Y. *et al.* Decitabine of reduced dosage in Chinese patients with myelodysplastic syndrome: a retrospective analysis. *PLoS One* **9**, e95473 (2014).
3. Fenaux, P., Mufti, G. J. & Hellstrom-Lindberg, E. *et al.* Efficacy of azacitidine compared with that of conventional care regimens in the treatment of higher-risk myelodysplastic syndromes: a randomised, open-label, phase III study. *Lancet Oncol* **10**, 223–232 (2009).
4. Kadia, T. M., Jabbour, E. & Kantarjian, H. Failure of hypomethylating agent-based therapy in myelodysplastic syndromes. *Semin Oncol* **38**, 682–692 (2011).
5. Gumireddy, K., Reddy, M. V. & Cosenza, S. C. *et al.* ON01910, a non-ATP-competitive small molecule inhibitor of Plk1, is a potent anticancer agent. *Cancer Cell* **7**, 275–286 (2005).
6. Chapman, C. M., Sun, X. & Roschewski, M. *et al.* ON 01910.Na is selectively cytotoxic for chronic lymphocytic leukemia cells through a dual mechanism of action involving PI3K/AKT inhibition and induction of oxidative stress. *Clin Cancer Res* **18**, 1979–1991 (2012).
7. Oussenko, I. A., Holland, J. F. & Reddy, E. P. *et al.* Effect of ON 01910.Na, an anticancer mitotic inhibitor, on cell-cycle progression correlates with RanGAP1 hyperphosphorylation. *Cancer Res* **71**, 4968–4976 (2011).
8. Prasad, A., Park, I. W. & Allen, H. *et al.* Styryl sulfonyl compounds inhibit translation of cyclin D1 in mantle cell lymphoma cells. *Oncogene* **28**, 1518–1528 (2009).
9. Jimeno, A., Li, J. & Messersmith, W. A. *et al.* Phase I study of ON 01910.Na, a novel modulator of the Polo-like kinase 1 pathway, in adult patients with solid tumors. *J Clin Oncol* **26**, 5504–5510 (2008).
10. Bowles, D. W., Diamond, J. R. & Lam, E. T. *et al.* Phase I study of oral rigosertib (ON 01910.Na), a dual inhibitor of the PI3K and Plk1 pathways, in adult patients with advanced solid malignancies. *Clin Cancer Res* **20**, 1656–1665 (2014).
11. Seetharam, M., Fan, A. C. & Tran, M. *et al.* Treatment of higher risk myelodysplastic syndrome patients unresponsive to hypomethylating agents with ON 01910.Na. *Leuk Res* **36**, 98–103 (2012).
12. Komrokji, R. S., Raza, A. & Lancet, J. E. *et al.* Phase I clinical trial of oral rigosertib in patients with myelodysplastic syndromes. *Br J Haematol* **162**, 517–524 (2013).
13. Silverman, L. R., Greenberg, P., Raza, A. *et al.* Clinical activity and safety of the dual pathway inhibitor rigosertib for higher risk myelodysplastic syndromes following DNA methyltransferase inhibitor therapy. *Hematol Oncol,* doi: 10.1002/hon.2137 (2014). [Epub ahead of print]
14. Valent, P., Horny, H. P. & Bennett, J. M. *et al.* Definitions and standards in the diagnosis and treatment of the myelodysplastic syndromes: Consensus statements and report from a working conference. *Leuk Res* **31**, 727–736 (2007).
15. Vardiman, J. W., Harris, N. L. & Brunning, R. D. The World Health Organization (WHO) classification of the myeloid neoplasms. *Blood* **100**, 2292–2302 (2002).
16. Greenberg, P. L., Tuechler, H. & Schanz, J. *et al.* Revised international prognostic scoring system for myelodysplastic syndromes. *Blood* **120**, 2454–2465 (2012).
17. Tohyama, K., Tohyama, Y. & Nakayama, T. *et al.* A novel factor-dependent human myelodysplastic cell line, MDS92, contains haemopoietic cells of several lineages. *Br J Haematol* **91**, 795–799 (1995).
18. Nakagawa, T. & Matozaki, S. The SKM-1 leukemic cell line established from a patient with progression to myelomonocytic leukemia in myelodysplastic syndrome (MDS)-contribution to better understanding of MDS. *Leuk Lymphoma* **17**, 335–339 (1995).
19. Pellegata, N. S., Antoniono, R. J. & Redpath, J. L. *et al.* DNA damage and p53-mediated cell cycle arrest: a reevaluation. *Proc Natl Acad Sci* **93**, 15209–15214 (1996).
20. Taylor, W. R. & Stark, G. R. Regulation of the G2/M transition by p53. *Oncogene* **20**, 1803–1815 (2001).
21. Katsoulidis, E., Li, Y. & Yoon, P. *et al.* Role of the p38 mitogen-activated protein kinase pathway in cytokine-mediated hematopoietic suppression in myelodysplastic syndromes. *Cancer Res* **65**, 9029–9037 (2005).
22. Pallela, V. R., Mallireddigari, M. R. & Cosenza, S. C. *et al.* Hydrothiolation of benzyl mercaptan to arylacetylene: application to the synthesis of (E) and (Z)-isomers of ON 01910·Na (Rigosertib®), a phase III clinical stage anti-cancer agent. *Org Biomol Chem* **11**, 1964–1977 (2013).
23. Kulasekararaj, A. G., Smith, A. E. & Mian, S. A. *et al.* TP53 mutations in myelodysplastic syndrome are strongly correlated with aberrations of chromosome 5, and correlate with adverse prognosis. *Br J Haematol* **160**, 660–672 (2013).
24. Ebert, B. L. Molecular dissection of the 5q deletion in myelodysplastic syndrome. *Semin Oncol* **38**, 621–626 (2011).
25. Cazzola, M., Della Porta, M. G. & Malcovati, L. The genetic basis of myelodysplasia and its clinical relevance. *Blood* **122**, 4021–4034 (2013).
26. Issa, J. P. The myelodysplastic syndrome as a prototypical epigenetic disease. *Blood* **121**, 3811–3817 (2013).
27. Navas, T. A., Mohindru, M. & Estes, M. *et al.* Inhibition of overactivated p38 MAPK can restore hematopoiesis in myelodysplastic syndrome progenitors. *Blood* **108**, 4170–4177 (2006).
28. Bhagat, T. D., Zhou, L. & Sokol, L. *et al.* miR-21 mediates hematopoietic suppression in MDS by activating TGF-beta signaling. *Blood* **121**, 2875–2881 (2013).
29. Follo, M. Y., Mongiorgi, S. & Bosi, C. *et al.* The Akt/mammalian target of rapamycin signal transduction pathway is activated in high-risk myelodysplastic syndromes and influences cell survival and proliferation. *Cancer Res* **67**, 4287–4294 (2007).
30. Boehrer, S., Ades, L. & Braun, T. *et al.* Erlotinib exhibits antineoplastic off-target effects in AML and MDS: a preclinical study. *Blood* **111**, 2170–2180 (2008).
31. Ruan, G. X. & Kazlauskas, A. Lactate engages receptor tyrosine kinases Axl, Tie2, and vascular endothelial growth factor receptor 2 to activate phosphoinositide 3-kinase/Akt and promote angiogenesis. *J Biol Chem* **288**, 21161–21172 (2013).
32. Dellinger, M. T. & Brekken, R. A. Phosphorylation of Akt and ERK1/2 is required for VEGF-A/VEGFR2-induced proliferation and migration of lymphatic endothelium. *PLoS One* **6**, e28947 (2011).

Acknowledgments

This study was supported by the National High Technology Research and Development Program of China ("863" program, Grant No. 2012AA02A505) and the National Natural Science Foundation of China (Grant No. 81270584, 81300389, 81100341 and 81470291).

Author contributions

X.F., L.X. and H.Q. designed this study and wrote this manuscript; X.F., H.Q., W.L.Y., Z.Z., L.L., S.W.H. and Z.Y. performed experiments; Z.Y.S., F.C.M. and G.J. analyzed the data; C.C.K., G.S.C., W.D. and Z.L.Y. manage patients and collected clinical samples.

Additional information

Competing financial interests: The authors declare no competing financial interests.

How to cite this article: Xu, F. *et al.* Rigosertib as a selective anti-tumor agent can ameliorate multiple dysregulated signaling transduction pathways in high-grade myelodysplastic syndrome. *Sci. Rep.* **4**, 7310; DOI:10.1038/srep07310 (2014).